J Solid State Electrochem (2008) 12:461–469
DOI 10.1007/s10008-007-0471-5

ORIGINAL PAPER

Counterion binding induces attractive interactions between negatively-charged self-assembled monolayer of 3-mercaptopropionic acid on Au(111) in reductive desorption

Yukio Kitagawa · Daisuke Hobara · Masahiro Yamamoto · Takashi Kakiuchi

Received: 15 July 2007 / Revised: 31 October 2007 / Accepted: 1 November 2007 / Published online: 5 December 2007

Abstract The electrochemical reductive desorption of the self-assembled monolayers of 3-mercaptopropionic acid in an aqueous alkaline solution gives a sharp peak with the full width at half maximum of about 20 mV irrespective of the type of cations in a linear scan voltammogram. This suggests that a strong attractive interaction exists between negatively charged carboxylate groups in the self-assembled monolayer surface due to the counterion binding, which not only simply stabilizes the adsorbed carboxylates but also makes the interaction between the adsorbed thiolates even attractive possibly by forming a two-dimensional ionic crystal. The effect of tetraalkylammonium ions on the shape of the voltammograms was also examined.

Keywords 3-Mercaptopropionic acid · Self-assembled monolayer · SAM · Reductive desorption · Voltammetry · Electrostatic interaction · Counterion binding · Au(111) · Two-dimensional ionic crystal

Introduction

Among alkanethiols and their thiol derivatives that form self-assembled monolayers (SAMs) on a metal surface, ω-carboxylalkanethiols [HOOC-$(CH_2)_n$SH] are unique in that their SAMs have distinctive surface properties, such as hydrophilicity, wettability, chemical reactivity, and an affinity towards positively charged proteins, e.g., cytochrome *c*. This fact makes HOOC-$(CH_2)_n$SH highly useful and attractive in designing SAMs for a variety of purposes [1–66]. One of the intriguing features of SAMs formed by HOOC-$(CH_2)_n$SH is that the reductive desorption of the SAM gives a sharp peak on a cyclic voltammogram recorded in an aqueous alkaline solution, e.g., 0.5 mol dm^{-3} KOH. The full width at half maximum (FWHM) is about 20 mV or even smaller, particularly when the number of methylene units, n, is as small as 1 or 2 [13–15]. This narrow FWHM suggests the presence of a strong lateral attractive interaction between adsorbed thiolates [67]. Such an attractive interaction might seem counterintuitive, as the surface pK value of the ω-carboxyl groups in the SAM is estimated to be about 7 ± 1 [2, 68–75], and all the ω-carboxyl groups are deprotonated to bear negative charges in an alkaline solution in recording voltammograms of reductive desorption. These negative charges are, in fact, neutralized by counterions that bind to the negatively charged SAMs, as confirmed by X-ray reflectivity [12], atomic force microscopy [76], quartz crystal microbalance [7], and Raman spectroscopy [32, 49, 77, 78].

However, the neutralization does not suffice to give rise to the attractive interaction among adsorbed thiolates. We suggested the possibility of the formation of a two-dimensional ionic crystal on the surface of ω-carboxylalkanethiol SAMs due to the counterion binding to explain the titration curves for the SAMs with an aqueous NaOH solution [73]. In the present paper, we report the effect of the nature of counterions on the reductive desorption for further examining the

Dedicated to Professor Oleg Petrii on the occasion of his 70th birthday.

Y. Kitagawa · D. Hobara · M. Yamamoto · T. Kakiuchi (✉)
Department of Energy and Hydrocarbon Chemistry,
Graduate School of Engineering, Kyoto University,
Kyoto 615-8510, Japan
e-mail: kakiuchi@scl.kyoto-u.ac.jp

possible formation of a quasi-two-dimensional crystal on the SAM.

Experimental

Materials

3-Mercaptopropionic acid (MPA) was purchased from Sigma-Aldrich (St. Louis, MO, USA) and was used without further purification. Monohydrates of LiOH, RbOH, and CsOH were purchased from Nakarai Tesque (Kyoto, Japan). Aqueous solutions of $(CH_3)_4NOH$ (15%), $(C_2H_5)_4NOH$ (10%), and $(C_4H_9)_4NOH$ (0.5 mol dm^{-3}) were purchased from Wako Pure (Osaka, Japan). All other chemicals were of reagent grade. Au substrates were prepared on freshly cleaved mica surface by vapor-deposition at a base pressure of 1×10^{-6} Torr. The temperature of a mica sheet was maintained at 580 °C during the deposition. Au-deposited mica sheets were annealed at 550 °C for 6 h before use. Other details of the preparation have been described previously [13]. Thiol-adsorbed Au electrodes were prepared by immersing a Au substrate in a 1-mmol dm^{-3} ethanol solution of a thiol overnight under nitrogen atmosphere.

Methods

Cyclic voltammograms (CVs) of the reductive desorption were recorded in 0.5 mol dm^{-3} MOH, where M is Li^+, Na^+, K^+, Rb^+, Cs^+, $(CH_3)_4N^+$, $(C_2H_5)_4N^+$, or $(C_4H_9)_4N^+$ using a Ag–AgCl–saturated KCl electrode as the reference electrode and a platinum wire as the counter electrode. The liquid junction between a test solution and the reference electrode was made through a glass frit filled with a saturated KCl solution. The applied potential reported hereafter is referred to the Ag–AgCl–saturated KCl electrode with this liquid junction. The current was taken to be negative when the reductive desorption proceeded. A gold substrate was mounted at the bottom of a cone-shaped cell using an O-ring of 4-mm diameter and a cramp [79]. The solution in the cell was deaerated by bubbling Ar for 10 min. All cyclic voltammetry measurements were made at 24±2 °C.

X-ray photoelectron spectroscopy (XPS) measurements were made at a base pressure of 1×10^{-8} Torr using a X-ray photoelectron spectrometer (ULVAC Phi, 5500MT) with an Mg K_α X-ray source. Binding energies were referenced to the Au $4f_{7/2}$ core level. Au substrates modified with MPA were rinsed with ethanol and, after drying in air, immersed in an aqueous alkaline solution for 10 min. The substrates were then rinsed again with ethanol prior to XPS measurements.

Scanning tunneling microscope (STM) images were recorded in an aqueous phosphate buffer solution using a PicoSPM-STM300A (Molecular Imaging) with a Nanoscope III (Digital Instruments, Tonawanda, NY, USA) as a controller equipped with a low-current unit (model: CSTMLC, Digital Instruments). Pt–Ir tips were electrochemically etched in 15% $CaCl_2$ and then coated with Apiezon wax. STM imaging was made in the constant-current mode. A Pt wire and a silver wire were used as counter and pseudoreference electrodes, respectively. The potential with respect to the silver wire was converted post hoc to that referred to a Ag–AgCl–satd.KCl electrode.

Results and discussion

Figure 1 shows CVs recorded at the scan rate of 20 mV^{-1} for the reductive desorption of MPA–SAMs from the Au surface recorded in aqueous solutions containing different alkali hydroxide, LiOH (curve a),

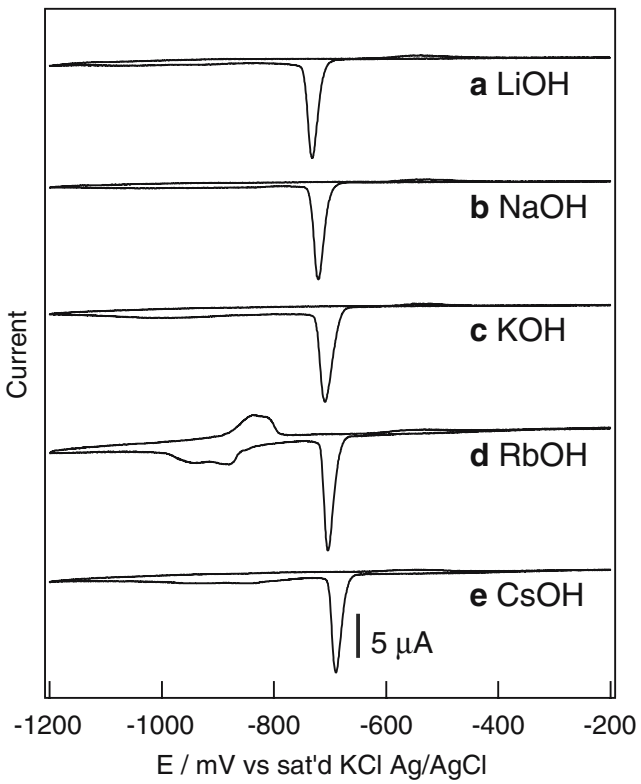

Fig. 1 CVs for reductive desorption of MPA SAMs in 0.5 mol dm^{-3} LiOH (**a**), NaOH (**b**), KOH (**c**), RbOH (**d**), and CsOH (**e**). Scan rate of the voltage: 20 $mV\ s^{-1}$

Table 1 Parameters of reductive desorption of MPA in aqueous alkaline solutions

Cations	Peak potential / mV	FWHM / mV	Charge / μC cm^{-2}
Li^+	-728 ± 5	18 ± 4	96 ± 2
Na^+	-708 ± 13	23 ± 4	93 ± 1
K^+	-702 ± 4	23 ± 4	91 ± 12
Rb^+	-706 ± 4	18 ± 2	95 ± 5
Cs^+	-681 ± 8	21 ± 4	77 ± 7

NaOH (curve b), KOH (curve c), RbOH (curve d), and CsOH (curve e). In each voltammogram, a sharp peak of the reductive desorption of adsorbed MPA SAMs appeared around -700 mV. A broad hump visible in the case of RbOH is probably due to the impurities originally contained in $RbOH{\cdot}H_2O$. Table 1 summarizes the values of peak potential, FWHM, and charge calculated from the peak area.

One of the most notable features in these voltammograms is the narrow FWHM of about 21 ± 3 mV irrespective of the type of the cation. This value is comparable to the value, 20 mV, found in the reductive desorption of the alkanethiolate SAMs having the number of a methylene moiety greater than 10, long enough for exhibiting strong lateral attractive interaction due to the van der Waals force between the tightly packed alkyl chains [67]. Similar narrow peaks have also been found in CV of the reductive desorption of other ω-functionalized alkanethiol SAMs having charged head groups, e.g., 2-mercaptoethanesulfonic acid (MES) [80], a mixture of MES and 2-aminoethanethiol [81, 82], and cysteine [83]. A common possible mechanism of all these cases is a strong lateral attraction between adsorbed molecules.

The observed narrow peak width in the present case therefore strongly suggests the presence of the attractive interaction between adsorbed MPA molecules in contact with an aqueous alkaline solution. We note that the charge neutralization itself is not enough to explain the narrow width because the adsorption in the absence of the lateral interaction leads to a much broader desorption peak; the FWHM is 120 mV in case of the Langmuir isotherm [67, 84].

Because the van der Waals interaction between adsorbed MPA is weak, other attractive interactions should exist, such as hydrogen bonding and electrostatic stabilization through counterion binding. In a strongly alkaline solution, it is highly probable that counter cations on the dissociated MPA SAM are ordered to form a quasi two-dimensional regular array. For example, if we assume a $(\sqrt{3} \times \sqrt{3})R30°$ structure of MPA on Au(111), an ideal 2D arrangement of counterions would be the same $(\sqrt{3} \times \sqrt{3})R30°$ structure, where each counterion occupies a three-fold hollow site of a triangle formed by three adsorbed MPAs. Unlike a crystal, however, the degree of ordering of the counterions and ω-carboxyl groups of the SAM is presumably not as regular as that of ionic crystals. Counterion binding to ω-carboxylate in the 16-mercaptohexadecanoinc acid SAM on Au(111) has been first confirmed by Li et al. [12] from X-ray reflectivity measurements, although no indication of in-plane order in the counterion multilayer was obtained. Using XPS, Himmel et al. found the 1:1 binding of K^+ to a carboxyterphenylmethanethiol SAM [85]. From XPS measurements, we found the ratios of the counterion to the S atom of adsorbed MPA were estimated to be 1.89, 1.50, and 1.26 for Na^+, K^+, and Cs^+, respectively. These values are greater than unity. However, considering the electron collection efficiency, which we did not take account of, we believe that these data support the 1:1 stoichiometry between alkali metal ions and adsorbed MPA molecules.

In Raman spectroscopy studies of the SAMs of MES on Ag, Kudelski found that, in aqueous alkaline solution, a MES SAM forms a salt-like MES monolayer with coadsorbed metal cations, which lose some hydration water molecules [77, 86], whereas the MPA monolayer is less ordered on polycrystalline Ag [32, 86]. Because the reductive desorption of MES from Au(111) gives 20 mV for FWHM for the peak on a voltammogram [81], it is likely that the ordering of MPA SAM on Au(111) in an aqueous alkaline solution is similar to that of MES to give a similar electrostatic interaction between negatively charged adsorbed thiols.

The role of counterion binding to the shape of the voltammograms was also obtained by measuring the reductive desorption in aqueous solutions at different pH values (Fig. 2). Lowering of pH caused a remarkable shift of the peak potential to the positive direction, which is related to the protonation equilibrium of the desorbed thiolates [87]. Simultaneously, the significant peak broadening is clearly discerned in the voltammograms. The change in FWHM is in parallel with the decrease in the capacitance [73] as shown in Fig. 3. The latter change reflects the protonation equilibrium of adsorbed MPA at the ω carboxyl group, as reported previously [73]. Obviously, the decrease in the number of counterions due to the protonation of a small fraction of the ω carboxyl group of adsorbed MPA results in the peak broadening. This suggests that the loss of

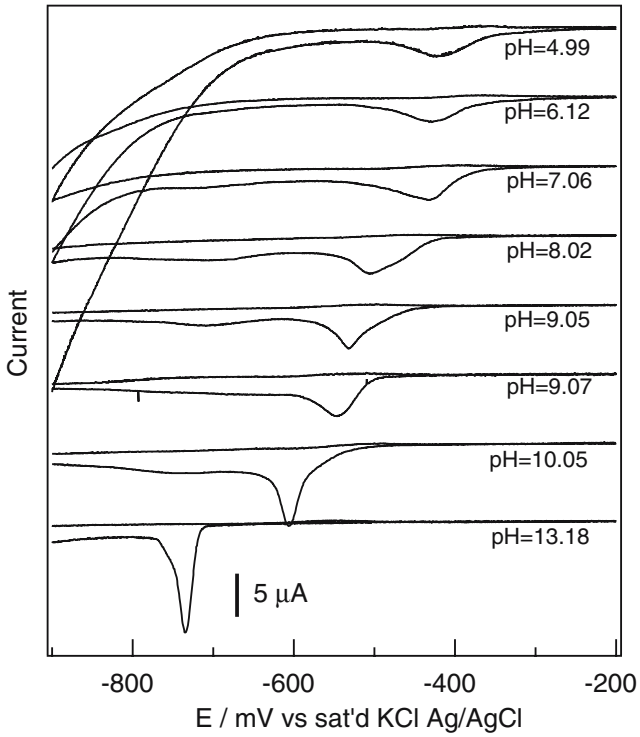

Fig. 2 CVs for reductive desorption of MPA SAMs in phosphate buffer of different pH values at the ionic strength of 0.2 mol dm^{-2}. The solution at pH = 13.18 is 0.2 mol dm^{-3} NaOH. Scan rate of the voltage: 20 mV s^{-1}

global regularity of the two-dimensional arrangement of the counterions drastically reduces the lateral attractive interaction.

The charge under the peak, 94 ± 2 μC cm^{-2}, did not depend on the type of counterions, with a possible exception of 77 μC cm^{-2} in the case of CsOH (Table 1). These values are greater than 74 μC cm^{-2} expected

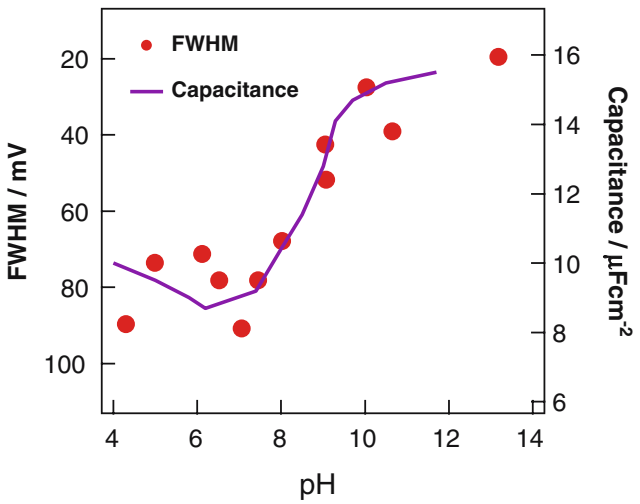

Fig. 3 Dependence of FWHM of the voltammetric peak in reductive desorption of MPA on pH (●). *Solid line* shows double-layer capacitance values in Kakiuchi et al. [73]

in the adsorption of thiolates forming $(\sqrt{3} \times \sqrt{3})R30°$ structure. In fact, from STM imaging shown below, the structure of adsorbed MPA SAMs of our sample is not exactly $(\sqrt{3} \times \sqrt{3})R30°$, but surface density of MPA is similar to that of $(\sqrt{3} \times \sqrt{3})R30°$. The contribution of the charging current to the total peak area in Table 1 is thus judged to be as large as one third of the peak area. Such a high fraction of charging current is associated with the strong dependence of desorption on the applied potential, which may be likened to the phase transition [67]. The large contribution of charging current to the reductive desorption is an indication of the presence of strong lateral interaction, presumably due to the two-dimensional crystal on the MPA SAM in contact with an aqueous alkaline solution.

The peak potential, E_p, slightly shifted from −728 mV for LiOH to −681 mV for CsOH when the ionic radius of the cation was increased. The position of the peak primarily reflects the adsorption Gibbs energy [88]. The positive shift of E_p means that adsorbed MPA molecules are more readily desorbed with increasing the ionic radius of alkali metal ions in the solution. A possible explanation is that the desorbed MPA dianions associate with alkali metal ions in the solution to form monovalent anions. Such ion-pair formation should facilitate the desorption to shift the peak potential to the positive direction. In other words, desorbed MPA dianions appear to be more effectively stabilized by Cs^+ than with strongly hydrated Li^+.

Effect of tetraalkylammonium ions for reductive desorption

In reductive desorption of the SAMs in an aqueous alkaline solution, counterions are supposed to be bound to the carboxylates exposed to the solution for charge neutralization without changing the two-dimensional arrangement of adsorbed MPA in the SAM. In this situation, the size of counterions should be important for the effective neutralization. For example, if the thiolate moiety of MPA takes a $(\sqrt{3} \times \sqrt{3})R30°$ structure on Au(111), it would be geometrically difficult for ions whose ionic radii is greater than Cs^+ to occupy interstitial sites, unlike the case of alkali metal ions. The radius of $(CH_3)_4N^+$ ion, 0.26 nm, is too large to sit in the center of triangle formed by three MPA moieties, while Cs^+, 0.17 nm, can do so. Presumably, the steric restriction forces tetraalkylammonium ions to be located above the surface of carboxyl groups, and the electrostatic stabilization would become more difficult with increasing the size of counterions. With this expectation, we examined the reductive desorption of MPA SAMs in aqueous solutions of $(CH_3)_4NOH$,

$(C_2H_5)_4NOH$, and $(C_4H_9)_4NOH$. Voltammograms for the reductive desorption in 0.5 mol dm^{-3} $(CH_3)_4NOH$, $(C_2H_5)_4NOH$, and $(C_4H_9)_4NOH$, are shown in Fig. 4. The desorption potential is about 100 mV more negative than those in alkali metal hydroxide solutions. In the case of $(CH_3)_4NOH$ and $(C_2H_5)_4NOH$, the peak split into two. This splitting was reproducible, though the relative peak heights varied from one sample to another. The charge calculated from the peak area was about 10% smaller than those recorded in alkali metal hydroxide solutions. Relevant parameters of these desorption peaks are summarized in Table 2.

In contrast to a simple expectation that the steric hindrance against the two-dimensional crystal causes broader desorption peaks, as are the cases at lower pH values in Fig. 2, the FWHM was very small, 16 mV, in the case of $(C_4H_9)_4NOH$, although the radius of $(C_4H_9)_4N^+$ is 0.7 nm [89]. On the other hand, the MPA moieties in the SAM in tetraalkylammonium hydroxide solutions should be fully dissociated, as the surface pK value is about 8 (Fig. 3). To neutralize this high surface charge density of about 70 μC cm^{-2}, a monolayer of counterions is not enough, unlike the case of alkali metal ions, and the double layer thickness should

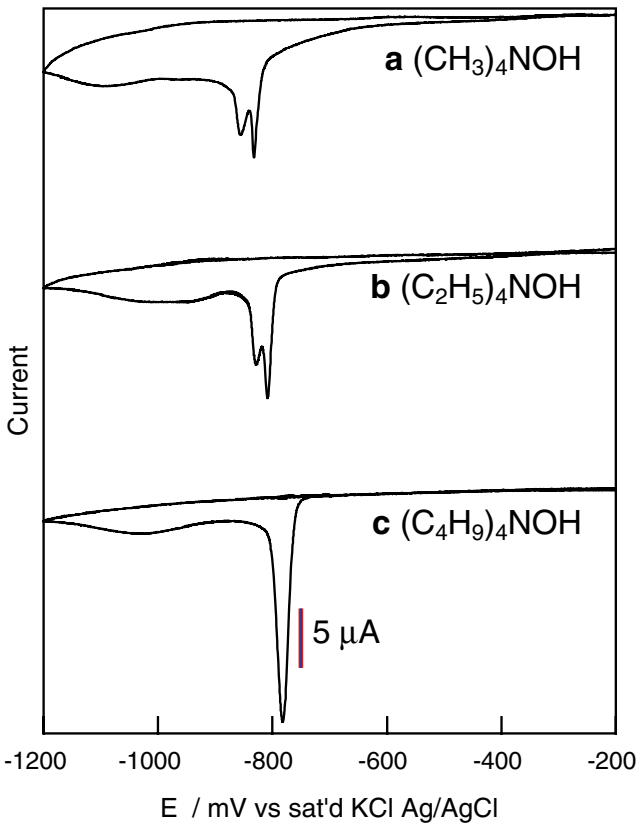

Fig. 4 CVs of the reductive desorption of MPA SAMs in 0.5 mol dm^{-3} aqueous $(CH_3)_4NOH$ (**a**), $(C_2H_5)_4NOH$ (**b**), and $(C_4H_9)_4NOH$ (**c**). Scan rate of the voltage: 20 mV s^{-1}

Table 2 Parameters of reductive desorption of MPA in 0.5 mol dm^{-3} aqueous tetraalkylammonium hydroxide

Cations	Peak potential / mV	FWHM / mV	Charge / μC cm^{-2}
$(CH_3)_4N^+$	-804 ± 15 -833 ± 17		72 ± 2
$(C_2H_5)_4N^+$	-779 ± 10 -808 ± 14		82 ± 10
$(C_4H_9)_4N^+$	-731 ± 12	16 ± 2	81 ± 12

be much thicker than the Debye length, 0.43 nm for 0.5 mol dm^{-3} in an aqueous solution at 25 °C.

The electrical double layer of an aqueous solution of $(C_4H_9)_4NCl$ or $(C_4H_9)_4NBr$ in contact with mercury or other metal electrodes is unique in that the adsorption of these ions is accompanied with coadsorption of anions [90], which can result in the capacitance pit of a few microfarads per square centimeter in differential capacitance vs potential curves [91]. The densely adsorbed multilayer of $(C_4H_9)_4N^+$ with inclusion of smaller anions is the most probable structure of the low capacitance value. Most of the studies of this kind have been conducted with tetraalkylammonium halides or sulfates. A similar low capacitance has also been found in the case of tetrabutylammonium hydroxide on gold [92]. Interestingly, the capacitance shows a very slow time dependence on the order of tens of minutes, which seems to be required for a long-range ordered multilayer structure [92].

It is therefore highly likely that, in the present case, the negatively charged MPA SAMs are overlaid with a multilayer of tetraalkylammonium ions because a monolayer of tetraalkylammonium ions is geometrically insufficient to neutralize the negative charges on the MPA SAM as described above. The reductive desorption of the MPA SAM should then be accompanied by the desorption of tetraalkylammonium ions. First, such a codesorption of tetraalkylammonium ions would make the desorption potential more negative, because of their hydrophobicity, as is the case of adsorption of organic compounds. Second, the desorption of the ordered multilayer should be cooperative to give a narrower peak width, as exemplified in the desorption in the presence of $(C_4H_9)_4N^+$ (Fig. 4). The desorption of the multilayer of counterions, not the desorption of MPA–SAM per se, probably determines the shape of the desorption peak. We note that a sharp desorption peak in capacitance vs potential curves has also been found in the desorption of $(C_4H_9)_4N^+$ from mercury [91], as well as from gold [92].

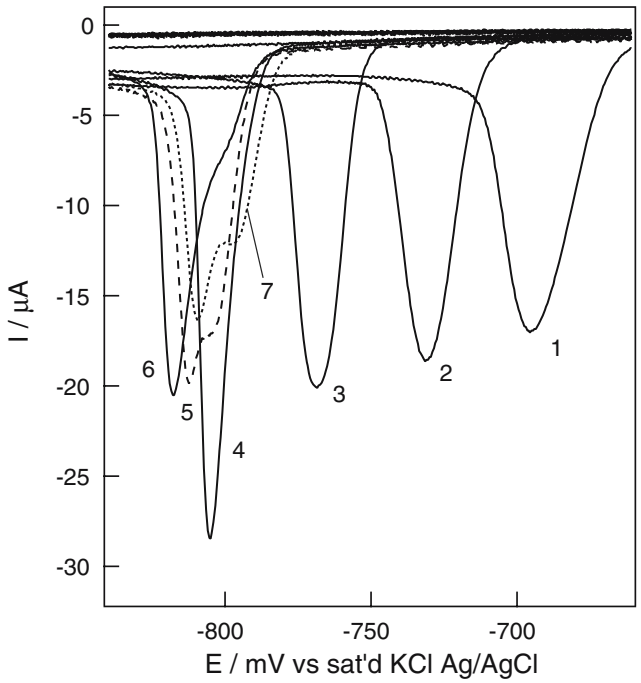

Fig. 5 Effect of mixing ration of KOH and $(C_2H_5)_4NOH$ on the desorption peak of MPA SAMs. KOH/$(C_2H_5)_4NOH$ = 1:0 (*curve 1*), 1:1 (*curve 2*), 1:9 (*curve 3*), 1:99 (*curve 4*), 1:1,000 (*curve 5*), 1:5,000 (*curve 6*), and 0:1 (*curve 7*). Scan rate of the voltage: 20 mV s^{-1}

The shift of the desorption potential to slightly positive potentials with increasing size of tetraalkylammonium ions (Fig. 4) can be interpreted in terms of the counterion binding to the desorbed MPA dianions, as is the case of the peak shift with cation size in Fig. 1.

The split of the peak in the case of $(CH_3)_4NOH$ and $(C_2H_5)_4NOH$ is possibly caused by the coadsorption of a contaminant, such as K^+, and $(CH_3)_4N^+$ or $(C_2H_5)_4N^+$ in the different region of the MPA SAM. To examine this possibility, the desorption of a MPA SAM was studied in mixed alkaline solutions of KOH and $(C_2H_5)_4NOH$. The results in Fig. 5 at different mixing ratios keeping the total hydroxide concentration constant at 0.5 mol dm^{-3} show that, with increasing the ratio of $(C_2H_5)_4NOH$, the desorption peak shifted to the negative potentials and the FWHM simultaneously narrowed up to the mixing ratio of 1:99 for KOH/$(C_2H_5)_4NOH$. A further increase in the ratio of $(C_2H_5)_4NOH$ results in the broadening (curve 5) and splitting of the peak into two (curves 6 and 7).

It is noteworthy that even the mixing ratio of 1:1 caused the sharpening of the peak and shifted the

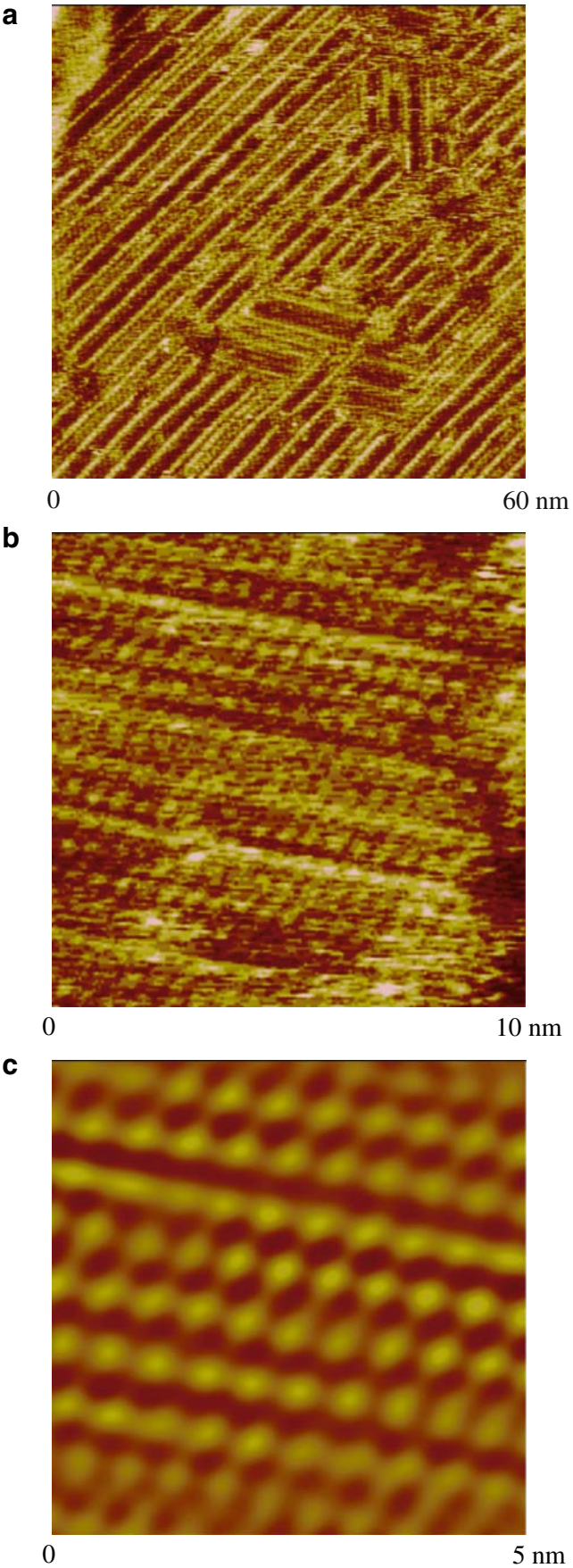

Fig. 6 STM images of an MPA SAM in a 30-mmol dm^{-3} phosphate buffer solution (pH = 7.15). **c** Part of the Fourier filtered image of **b**. Electrode voltage, −0.3 V; bias voltage, 0.7 V; set point, 650 pA

peak to the negative potential by 35 mV. This suggests the preferential adsorption of $(C_2H_5)_4N^+$ ions on the MPA surface. At the ratio of 1:99, the majority of the counterions is $(C_2H_5)_4N^+$. The shoulder or splitting peaks in Figs. 4 and 5 are therefore not caused by the coadsorption of $(C_2H_5)_4N^+$ and K^+ but are indicative of the inhomogeneity in $(C_2H_5)_4N^+$ multilayer.

STM imaging of the structure of MPA SAM

Figure 6 shows in-situ STM images of a MPA SAM recorded in 30 mmol dm^{-3} phosphate buffer at pH = 7.15 at $E = -0.3$ V. A clear pinstripe pattern is seen in Fig. 6a. An enlarged view in Fig. 6b shows that four lines of dots form a bundle corresponding to one stripe. A Fourier filtered image in Fig. 6c shows that the packing density is close to $(\sqrt{3} \times \sqrt{3})R30°$.

It has been known that MPS SAMs on Au(111) exhibit different types of two-dimensional arrangements in STM imaging, $p \times \sqrt{3}$ [93] with p = 3.6–4.8 [94], a rhombic (3 × 3) with the packing arrangement of MPA close to that of $(\sqrt{3} \times \sqrt{3})R30°$ [95], and $(2\sqrt{3} \times \sqrt{7})$ for the double row and $(2\sqrt{3} \times 4)$ symmetry [94].

As the structure of MPA SAMs depends on the method of preparation and the time, in particular, after the initial formation of the monolayer [32, 77, 78], it is not surprising to see several different structures of MPA SAMs. These different structures do not, however, seem to be reflected in the reductive desorption behavior because the reductive desorption of MPA SAMs in aqueous alkaline solutions always gives a single peak with similar FWHM values. More detailed studies using chronoamperometry with continuous monitoring of high-speed STM imaging will be able to reveal the correspondence between the molecular-level two-dimensional arrangements of MPA in SAMs and reductive desorption characteristics.

Conclusions

A narrow peak width in reductive desorption of adsorbed MPA from Au(111) in an aqueous alkaline solution, irrespective of the type of cations, is strongly indicative of the presence of strong electrostatic stabilization of the adsorbed MPA molecules. The formation of the two-dimensional ionic lattice has been proposed as a putative mechanism for the strong lateral attractive interaction between the adsorbed MPA molecules. In the reductive desorption in an aqueous tetraalkylammonium hydroxide, the cooperative desorption of layered tetraalkylammonium ions is likely to determine the location and shape of the desorption peak in voltammograms. This shows an intriguing example of charge neutralization by bulky counterions at the interface. The present counter-binding effect on the reductive desorption is a special case showing the significance of the electrostatic interaction of adsorbed cations and anions in electrode reactions, which is one of the subjects pioneered by Petrii and coworkers [96–98] in relation to the Frumkin effect.

Acknowledgement We greatly acknowledge the comments by Koichi Aoki on the possible formation of a two-dimensional ionic crystal in reductive desorption of MPA SAMs.

References

1. Bain CD, Evall J, Whitesides GM (1989) J Am Chem Soc 111:7155–7164
2. Bain CD, Whitesides GM (1989) Langmuir 5:1370–1378
3. Laibinis PE, Fox MA, Folkers JP, Whitesides GM (1991) Langmuir 7:3167–3173
4. Evans SD, Sharma R, Ulman A (1991) Langmuir 7:156–161
5. Laibinis PE, Whitesides GM (1992) J Am Chem Soc 114: 1990–1995
6. Folkers JP, Laibinis PE, Whitesides GM (1992) Langmuir 8:1330–1341
7. Wang J, Frostman LM, Ward MD (1992) J Phys Chem 96: 5224
8. Offord DA, John CM, Griffin JH (1994) Langmuir 10: 761–766
9. Offord DA, John CM, Linford MR, Griffin JH (1994) Langmuir 10:883–889
10. Lee TR, Carey RL, Biebuyck HA, Whitesides GM (1994) Langmuir 10:741–749
11. Zhong CJ, Porter MD (1994) J Am Chem Soc 116:11616–11617
12. Li J, Liang KS, Scoles G, Ulman A (1995) Langmuir 11: 4418–4427
13. Imabayashi S, Iida M, Hobara D, Feng ZQ, Niki K, Kakiuchi T (1997) J Electroanal Chem 428:33–38
14. Imabayashi S, Hobara D, Kakiuchi T, Knoll W (1997) Langmuir 13:4502–4504
15. Nishizawa M, Sunagawa T, Yoneyama H (1997) J Electroanal Chem 436:213–218
16. Imabayashi S, Gon N, Sasaki T, Hobara D, Kakiuchi T (1998) Langmuir 14:2348–2351
17. Hobara D, Ota M, Imabayashi S, Niki K, Kakiuchi T (1998) J Electroanal Chem 444:113–119
18. Hobara D, Ueda K, Imabayashi S, Yamamoto M, Kakiuchi T (1999) Electrochemistry 67:1218–1220
19. Hobara D, Sasaki T, Imabayashi S, Kakiuchi T (1999) Langmuir 15:5073–5078
20. Dong YZ, Shannon C (2000) Anal Chem 72(11):2371–2376
21. Kawaguchi T, Yasuda H, Shimazu K, Porter MC (2000) Langmuir 16:9830–9840

22. Gobi KV, Mizutani F (2000) J Electroanal Chem 484(2): 172–181
23. Hobara D, Uno Y, Kakiuchi T (2001) Phys Chem Chem Phys 3:3437–3441
24. Munakata H, Kuwabata S, Ohko Y, Yoneyama H (2001) J Electroanal Chem 496:29–36
25. Kakiuchi T, Iida M, Gon N, Hobara D, Imabayashi S, Niki K (2001) Langmuir 17:1599–1603
26. Imabayashi S, Hobara D, Kakiuchi T (2001) Langmuir 17:2560–2563
27. Azzaroni O, Vela ME, Martin H, Creus AH, Andreasen G, Salvarezza RC (2001) Langmuir 17(21):6647–6654
28. Gorman CB, He YF, Carroll RL (2001) Langmuir 17: 5324–5328
29. Satjapipat M, Sanedrin R, Zhou FM (2001) Langmuir 17: 7637–7644
30. Shimazu K, Kawaguchi T, Isomura T (2002) J Am Chem Soc 124:652–661
31. Shimazu K, Hashimoto Y, Kawaguchi T, Tada K (2002) J Electroanal Chem 534:163–169
32. Kudelski A (2002) Surf Sci 502:219–223
33. Vericat C, Lenicov FR, Tanco S, Andreasen G, Vela ME, Salvarezza RC (2002) J Phys Chem B 106:9114–9121
34. Hobara D, Imabayashi S, Kakiuchi T (2002) Nano Lett 2:1021–1025
35. Nakamura T, Kimura R, Sakai H, Abe M, Kondoh H, Ohta T, Matsumoto M (2002) Appl Surf Sci 202:241–251
36. Chen X, Ferrigno R, Yang J, Whitesides GM (2002) Langmuir 18:7009–7015
37. Roux S, Duwez AS, Demoustier-champagne S (2003) Langmuir 19:306–313
38. Oyamatsu D, Kanaya N, Hirano Y, Nishizawa M, Matsue T (2003) Electrochemistry 71:439–441
39. Burshtain D, Mandler D (2004) ChemPhysChem 5: 1532–1539
40. Tian Y, Mao LQ, Okajima T, Ohsaka T (2004) Anal Chem 76:4162–4168
41. Freire RS, Kubota LT (2004) Electrochim Acta 49: 3795–3800
42. Campuzano S, Pedrero M, Villena FJM, Pingarron JM (2004) Electroanalysis 16:1385–1392
43. Liu Y, Yang M, Zheng Z, Zhang B (2005) Electrochem Commun 7:344–348
44. Mena ML, Carralero V, Gonzalez-Cortes A, Yanez-Sedeno P, Pingarron JM (2005) Electroanalysis 17:2147–2155
45. Burshtain D, Mandler D (2005) J Electroanal Chem 581: 310–319
46. Chen H, Heng CK, Puiu PD, Zhou XD, Lee AC, Lim TM, Tan SN (2005) Anal Chim Acta 554:52–59
47. Zhang XH, Wang SF, Shen QH (2005) Microchim Acta 149:37–42
48. Carvalhal RT, Freire RS, Kubota LT (2005) Electroanalysis 17:1251–1259
49. Kudelski A, Michota A, Bukowska J (2005) J Raman Spectrosc 36:709–714
50. Wrzosek B, Bukowska J, Kudelski A (2005) Vibr Spectrosc 39:257–261
51. Albrecht T, Li W, Ulstrup J, Haehnel W, Hildebrandt P (2005) ChemPhysChem 6:961–970
52. Ujihara M, Imae T (2006) J Colloid Interface Sci 293: 333–341
53. Imabayashi S, Kashiwa M, Watanabe M (2006) Electrochemistry 74:186–188
54. Kado S, Murakami T, Kimura K (2006) Anal Sci 22: 521–527
55. Xu JS, Bowden EF (2006) J Am Chem Soc 128:6813–6822
56. Kubo I, Nakane Y, Maehara N (2006) Electrochim Acta 51(24):5163–5168
57. Ito E, Nakamura F, Kanai K, Ouchi Y, Seki K, Hara M (2006) Jpn J Appl Phys 45:409–412
58. Cecchet F, Marcaccio M, Margotti M, Paolucci F, Rapino S, Rudolf P (2006) J Phys Chem B 110:2241–2248
59. Yue HJ, Waldeck DH, Petrovic J, Clark RA (2006) J Phys Chem B 110:5062–5072
60. Phong PH, Yamamoto M, Kakiuchi T (2006) Sci Technol Adv Mater 7:552–557
61. Zhang JD, Chi QJ, Ulstrup J (2006) Langmuir 22: 6203–6213
62. Yu JJ, Tan YH, Li X, Kuo PK, Liu GY (2006) J Am Chem Soc 128:11574–11581
63. Limbut W, Kanatharana P, Mattiasson B, Asawatreratanakul P, Thavarungkul P (2006) Biosens Bioelectron 22:233–240
64. Kim SJ, Gobi KV, Tanaka H, Shoyama Y, Miura N (2006) Chem Lett 35:1132–1133
65. Carot ML, Macagno VA, Paredes-olivera P, Patrito EM (2007) J Phys Chem C 111:4294–4304
66. Campuzano S, Gamella M, Serra B, Reviejo AJ, Pingarron JM (2007) J Agric Food Chem 55(6):2109–2114
67. Kakiuchi T, Usui H, Hobara D, Yamamoto M (2002) Langmuir 18:5231–5238
68. Creager SE, Clarke J (1994) Langmuir 10:3675–3683
69. Hu K, Bard AJ (1997) Langmuir 13:5114–5119
70. Vezenov DV, Noy A, Rozsnyai LF, Lieber CM (1997) J Am Chem Soc 119:2006–2015
71. Smalley JF, Chalfant K, Feldberg SW, Nahir TM, Bowden EF (1999) J Phys Chem B 103:1676–1685
72. White HS, Peterson JD, Cui QZ, Stevenson KJ (1998) J Phys Chem B 102:2930–2934
73. Kakiuchi T, Iida M, Imabayashi S, Niki K (2000) Langmuir 16:5397–5401
74. Kim K, Kwak J (2001) J Electroanal Chem 512:83–91
75. Schweiss R, Werner C, Knoll W (2003) J Electroanal Chem 540:145–151
76. Kane V, Mulvaney P (1998) Langmuir 14:3303–3311
77. Kudelski A (2002) Langmuir 18:4741–4747
78. Kudelski A (2003) J Raman Spectrosc 34:853–862
79. Widrig CA, Chung C, Porter MD (1991) J Electroanal Chem 310:335–359
80. Hobara D, Yamamoto M, Kakiuchi T (2001) Chem Lett 374–375
81. Ooi Y, Hobara D, Yamamoto M, Kakiuchi T (2005) Langmuir 21:11185–11189
82. Phong PH, Ooi Y, Hobara D, Nishi N, Yamamoto M, Kakiuchi T (2005) Langmuir 21:10581–10586
83. Zhang J, Chi Q, Nielsen JU, Friis EP, Andersen JET, Ulstrup J (2000) Langmuir 16:7229–7237
84. Angerstein-Kozlowska H, Klinger J, Conway BE (1977) J Electroanal Chem 75:45–60
85. Himmel HJ, Terfort A, Woll C (1998) J Am Chem Soc 120:12069–12074
86. Kudelski A, Pecul M, Bukowska J (2002) J Raman Spectrosc 33:796–800

87. Munakata H, Oyamatsu D, Kuwabata S (2004) Langmuir 20:10123–10128
88. Hatchett DW, Uibel RH, Stevenson KJ, Harris JM, White HS (1998) J Am Chem Soc 120:1062–1069
89. Dong Y, Xu Z (1999) Langmuir 15:4590–4594
90. Hayter JB, Hunter RJ (1972) J Electroanal Chem 37: 71–80
91. Wandlowski T, de Levie R (1992) J Electroanal Chem 329:103–127
92. Tymosiak-Zielinska A, Borkowska Z (2001) Electrochim Acta 46:3073–3082
93. Giz MJ, Duong B, Tao NJ (1999) J Electroanal Chem 465: 72–79
94. Petri M, Kolb DM, Memmert U, Meyer H (2003) Electrochim Acta 49:175–182
95. Sawaguchi T, Sato Y, Mizutani F (2001) J Electroanal Chem 507:256–262
96. Nikolaeva-Fedorovich VN, Fokina LA, Petrii OA (1958) Dokl Akad Nauk SSSR 122:639–642
97. Nikolaeva-Fedorovich VN, Damaskin BB, Petrii OA (1960) Coll Czech Chem Commun 25:2982–2992
98. Frumkin AN, Petrii OA (1961) Dokl Akad Nauk SSSR 136:1158–1161